Type of contribution:
Editorial
▶ Research Paper
Case Study
Review Paper
Scientific Data
Report of Tech. Application

e-issn. 2798-5245
Mechanical Engineering for Society and Industry
Vol. 4, No. 2 (2024) pp 198-209
https://doi.org/10.31603/mesi.12373

Experimental investigations of number of blades effect on archimedes spiral wind turbine performance

An update of this article is available in Vol. 5 No. 1 (2025), pp. 286-287.
doi: 10.31603/mesi.13996

Agus Dwi Korawan[1*], **Rosadila Febritasari**[2]

[1] Mechanical Engineering, Sekolah Tinggi Teknologi Ronggolawe Cepu, **Indonesia**
[2] Mechanical Engineering, Institut Teknologi Nasional Malang, **Indonesia**

✉ ad_korawan@yahoo.co.id

This article contributes to:
7 AFFORDABLE AND CLEAN ENERGY
SUSTAINABLE DEVELOPMENT GOALS

Highlights:
- Archimedes Spiral Wind Turbine (ASWT) with archimedean spiral blade is investigated in terms of blade number,
- Aeromodelling performance of ASWT in generating power is depended on blade number.
- The number of blades can affect the power produced.

Abstract

This study investigates the effect of blade number on the performance of Archimedes Spiral Wind Turbines (ASWT), a low-speed axial flow turbine with an Archimedean spiral blade design. Experimental tests and numerical simulations were conducted to evaluate power generation and fluid flow behavior. Results revealed that a three-blade ASWT achieved optimal performance, producing 158.5% more power than the four-blade configuration. The findings highlight the significant influence of blade number on ASWT efficiency, offering insights for improving wind turbine design in urban renewable energy applications.

Keywords: Archimedes wind turbine; CFD; Spiral blade; Wind energy; Wind tunnel

1. Introduction

Currently, non-renewable energy sources have been scarce which hard to fulfill human needs especially electricity [1]. Therefore, scientists and researchers try to explore new and renewable energy sources [2]–[7]. Wind energy has become an alternative renewable energy source to produce electrical energy with the help of wind turbines which gather mechanical energy from the wind as torque and speed [8], [9]. The popular wind turbine designs that are usually known are Vertical Axis Wind Turbines (VAWT) and Horizontal Axis Wind Turbines (HAWT). Compared to the VAWT, the HAWT could produce larger power energy 259.491 kW and 271.447 kW at a wind speed of 5.86 m/s and 6.13 m/s, respectively [10]. The problem that should be solved is that both wind turbines are large-size turbines that are difficult to install and maintain, which means the installation processes need additional machinery to carry the heavy turbine and adjust the blade on the tall tower [11], [12]. In urban environments, where space constraints and installation challenges are prominent, traditional HAWTs and VAWTs become less practical due to their large size and maintenance requirements [13]. This has led to the exploration of alternative wind turbine designs such as the Archimedes Spiral Wind Turbine (ASWT), which offers a more compact and adaptable solution.

The ASWT is one of the wind turbine designs that is suitable for society who want to install the ASWT in their homes [14]. The ASWT is categorized as a horizontal axis wind turbine (HAWT) and constructed with a unique spiral blade based on Archimedes' principle so it can automatically align to the direction of the wind [15], [16]. The ASWT can be rotated in low-speed wind without

Article info
Submitted: 2024-09-24
Revised: 2024-12-16
Accepted: 2024-12-17

Publisher
Universitas Muhammadiyah Magelang

any yaw apparatus to produce more energy than HAWT and VAWT [17]–[19]. Its low-speed rotation capability, combined with its ability to function without complex alignment systems, makes the ASWT particularly effective in urban areas with turbulent and inconsistent wind conditions. Additionally, its compact design allows for easier installation and integration into urban infrastructure, such as rooftops and small community energy systems. This wind turbine become interesting to investigate because the different designs of blades can provide different performances, so the researchers consider these to obtain the optimal design to improve flow properties through the rotor blades [20].

First, the previous researchers had designed the ASWT with opening angle variations. The opening angle effect on the turbine's performance which had been conducted by Hamid et al. [21], showed that 60° can generate the best performance. A study by Kamal et al. [22] showed that the performance coefficient (C_p) of modified ASWT is 28,6% greater than the conventional ASWT. Siswantara et al. [23] conducted experimental analysis on the ASWT with an angle between 36° and 44°. The work showed that the angle had more effect to generate more power, but the turbine efficiency was less. Bhattarai et al. [24] numerically analyzed the power output and power coefficient of ASWT with 112.5 mm of pitch and 60 degrees of opening angle. At 12 m/s of wind speed, the maximum power output is 4.74 W and the maximum power coefficient is 0.25 at the tip speed ratio of 1.5. Eva et al. [25] stated that coefficient of lift (C_L) increased as the opening angle increased. Labib et al. [26] who analyzed the power and torque coefficient (C_t) of ASWT with different blade angle showed the C_t decrease when the blade angle increase. Mohamed et al., [27] found that the variable opening angle can produce 14.7% of power which is higher than the fixed-angle design. Khan et al. [28] investigated how varying the number of blades influences key performance parameters, including pressure, torque, mechanical power, and efficiency in ANSYS fluid flow under steady turbulent conditions. The findings indicated that an optimal design can be determined by maximizing power output through adjustments to the turbine's parameters, especially the number of blades. Kashyap et al. [29] analyzed the operational potential and willingness of Gharat (watermill) owners in the Western Himalayan region, based on data from 76 locations, to install turbines for electricity generation, concluding that converting existing watermills into electricity generators using Archimedes screw turbines is both feasible and cost-effective.

Other studies explored the aerodynamic effects of blade profiles [30]. The ASWT has a spiral blade that can generate greater output and performance coefficient than the propeller turbine [31]. The Archimedes wind turbine (AWT) designs with aerofoil blade and spiral blade were analyzed by Rao [32]. This study was conducted based on the Finite element method (FEM) which showed that the torque increased significantly with an aerofoil blade at a slower speed than a spiral blade. Ostia et al. [33] compared the ASWT and Savonius wind turbines to investigate the performance of different blade construction at a certain wind speed. The study concluded that the ASWT gives a good performance and could generate 5.10 W of power than the Savonius wind turbine which only produces 1.23 W of power. Kashyap et al. [34] investigated the potential of Archimedes screw turbines for electricity generation in low-head, low-flow-rate sites, particularly by optimizing screw configurations in terms of screw angle, flow rate, and RPM, and revealed that the efficiency of the turbine can reach approximately 90% under optimal conditions, specifically with a screw angle of 25° or less, a flow rate of below 1.5 L/s, and an optimized RPM to minimize frictional and overflow losses. Thakur et al. [35] investigated the efficiency, power output, and speed of Archimedes Screw Turbines (AST) at different tilt angles, flow rates, and loads, using experimental testing to determine the optimal performance, with results showing maximum efficiency at 22 degrees, power output at 25 degrees, and speed at 25 degrees. Lee et al. [36] explored the performance of small-scale Archimedes Screw Turbines (AST) for low-flow rivers in Sarawak, Malaysia, using a laboratory-tested prototype to analyze the effects of water velocity and inclination angle on RPM, torque, and efficiency, finding an optimal 45-degree angle with a water velocity of 1.0–1.5 m/s, generating maximum power of 1.54 kW and 94.6% efficiency, supported by statistical validation.

However, the number of blades and its impact on ASWT performance have yet to be systematically studied, leaving a critical research gap. This study addresses this gap by experimentally investigating ASWTs with different blade numbers using wind tunnel tests, supported by numerical simulations with CFD to analyze fluid flow behavior. The findings aim to enhance ASWT designs for optimized energy generation in urban environments, providing renewable energy solutions that are both efficient and accessible. By emphasizing blade number comparisons and combining experimental and simulation approaches, this work offers a novel perspective on ASWT optimization, bridging gaps in prior research and advancing renewable energy technologies for urban applications.

2. Methods

2.1. Experiment Method

The experiment was conducted in Ethe nergy Laboratory, Mechanical Engineering, Malang National Institute of Technology as shown in **Figure 1**. This wind tunnel consists of a Drum Blower Model FA-40Y, 130 watts of centrifugal fan with 1400 rotation per minute. The construction of the wind tunnel is 100 cm in length and 45 cm in diameter which was made from steel sheets. The test section has an acrylic sheet to see the specimens inside. The instruments used, as shown in **Figure 2**, include the GUI Trainer turbine for measuring parameters such as angle of attack, force, rotation per minute, wind speed, voltage, current, and power. These instruments underwent rigorous calibration to ensure accuracy, achieving a margin of error within ±5% for all measured values, thereby providing reliable data for analysis. The calibration involved using standard reference devices for wind speed and electrical measurements, ensuring consistency across repeated trials.

Figure 1. Experimental setup

The choice of specific wind speeds and blade configurations was informed by prior research and practical considerations. Wind speeds ranging from 3 to 12 m/s were selected to simulate typical urban wind conditions where ASWTs are deployed. These speeds represent a balance between real-world applicability and the operational limits of the wind tunnel. The blade configurations (n = 3 and n = 4) were chosen based on their prevalence in existing ASWT designs, as they are commonly associated with efficient energy conversion in low-speed wind environments. This study focuses on these configurations to determine their aerodynamic performance and validate whether they represent optimal designs for urban renewable energy solutions.

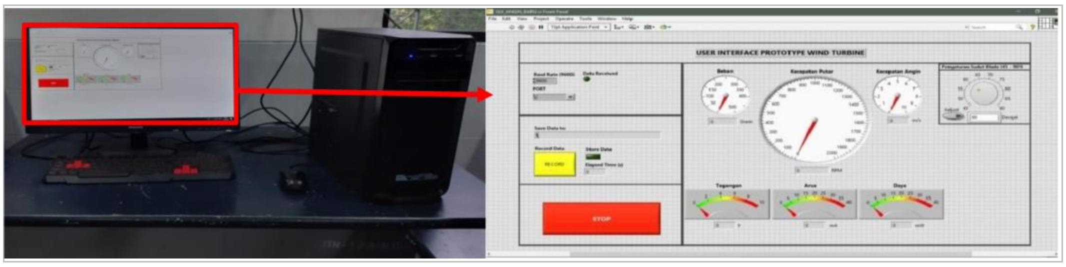

Figure 2. GUI Trainer Turbine is run in the computer

The ASWT is manufactured by 3D printing Ender 5 Pro from Polylactic Acid (PLA) material. The blade thickness is 2 mm, the inner shaft diameter (d_i) is 10 mm, and the outer diameter (d_o) is 16 mm that can be seen in **Figure 3**. The blade configurations of 3 blades and 4 blades were chosen based on their prevalence in prior studies and their potential for performance optimization. These configurations represent typical designs for ASWTs, allowing for a meaningful comparison to existing literature. In this study, the ASWT design with 3 blades and 4 blades was investigated experimentally in the wind tunnel. The

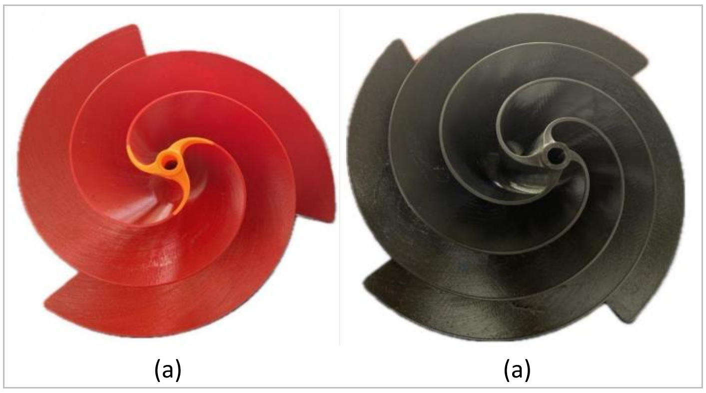

Figure 3. The ASWT design with (a) 3 blades and (b) 4 blades

ASWT is installed in the wind tunnel and fitted in the metal rotor hub. The wind speed is adjusted at 7 m/s. The suspended weight was set at 10 grams. In this experimental work, the torque generated is calculated to obtain the power coefficient, torque coefficient, and tip speed ratio (TSR). Those parameters are observed from the Eqs. 1) to (4).

The torque generated:

$$T = \frac{g \times r(W - L_c)}{1000} \tag{1}$$

The power coefficient:

$$C_p = \frac{2T\omega}{\rho A V^3} \tag{2}$$

The torque coefficient:

$$C_T = \frac{4T}{\rho A V^2 D} \tag{3}$$

The tip speed ratio:

$$TSR = \frac{\omega D}{2V} \tag{4}$$

where T is the generated torque, g is the gravitational acceleration, W is the suspended wieght in grams, L_c is the load cell reading in grams, and r is the shaft radius.

2.2. Simulation method

2.2.1. The archimedes spiral wind turbine (ASWT) design

This study uses wind turbines with spiral blades that are configured to the Archimedes principle. The ASWT is designed by CAD Software and the geometrical parameters are shown in Figure 4. It was varied by the number of blades (n = 3,4) with 65° of opening angle, so two designs were investigated to obtain the aerodynamic performance of fluid flow through the blade. The dimensions of the ASWT are 300 mm in diameter and 250 mm in motor streamwise length.

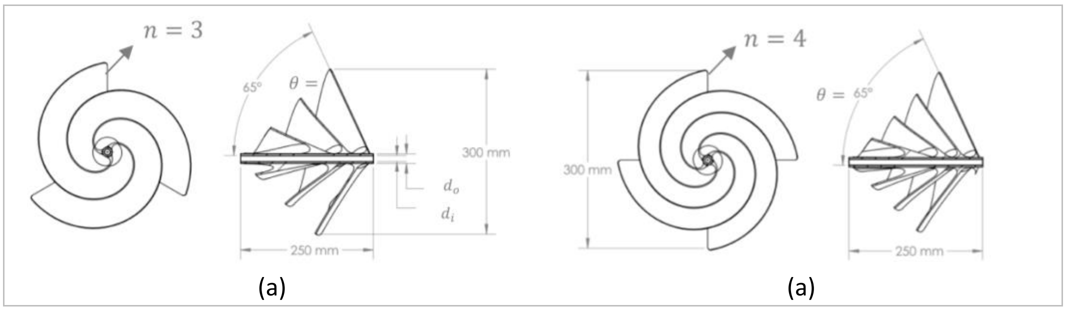

Figure 4. Geometrical parameters of the ASWT with (a) 3 blades and (b) 4 blades

2.2.2. Mesh generation

The ASWT model is imported to simulation software for setting the computational domain. The boundary condition is adjusted for separating the fluid and solid domains, as illustrated in Figure 5. The fluid domain boundary is shaped as a cylindrical domain that has a diameter twice the turbine diameter (2D) and consists of 2D upwind and 5D downwind. The mesh is designed with structured and unstructured elements to effectively capture the complex flow interactions around the turbine blades. Structured mesh elements are applied near the blade surfaces to accurately model boundary layer behavior, while unstructured elements are used in the outer fluid domain to accommodate the cylindrical geometry. The mesh is generated with a 10 mm mesh size, as this size balances

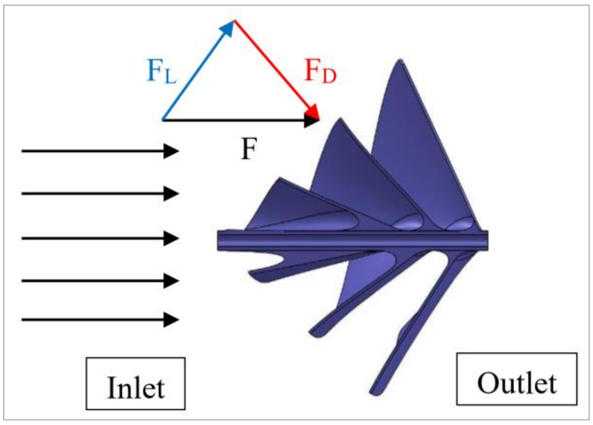

Figure 5. The illustration of aerodynamic force analysis on the ASWT rotor

computational efficiency and accuracy in capturing flow dynamics around the turbine. A smaller mesh size was tested but showed minimal gains in accuracy compared to the significantly increased computational cost. The element quality achieved was 0.83 on average, ensuring reliable simulation results. The nodes and elements numbers can be seen in **Table 1**.

Table 1. The elements and nodes of mesh contained in ASWT models

Blade number	Angle	Mesh Size (mm)	Nodes	Elements	Rationale for Mesh Size and Parameters
$n = 3$	$\theta = 65°$	10	128.364	675.892	Optimized for computational efficiency and sufficient detail
$n = 4$	$\theta = 65°$	10	153.370	799.341	Maintains consistency across designs for valid comparison

2.2.3. Boundary Condition

The simulation used velocity inlet and pressure outlet conditions to replicate wind flow through the turbine, as shown in **Figure 6** and **Figure 7**. The turbulence model employed was the SST k-ω model, chosen for its accuracy in predicting separation and adverse pressure gradients relevant to the ASWT design. The simulations were run until convergence, with residuals set to a threshold of 10^{-6}, ensuring accurate and stable results. Additional parameters, including second-order schemes for pressure and momentum discretization, were implemented to enhance solution fidelity.

Figure 6. Boundary conditions

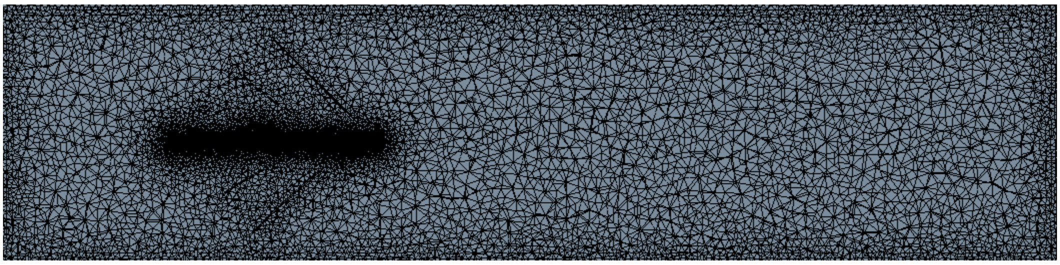

Figure 7. Sectional view of mesh

2.2.4. CFD turbulence model and simulation

The ASWT's aerodynamic performance is investigated from the fluid flow motion which can be predicted by choosing the suitable model solution which is the Reynolds Average Navier Stokes (RANS) equation. The illustration of the airflow across the ASWT is shown in **Figure 5**. The RANS equation is calculated by Newton's second law on the fluid particle based on time, and the influence of viscous force is taken into the actual fluid flow. The models are calculated based on the continuity and momentum equation, as shown in Eqs. (5) and (6), respectively.

Continuity equation:

$$\frac{\partial \overline{U}_i}{\partial x_i} = 0 \tag{5}$$

Momentum equation

$$\frac{\partial \overline{U}_i \overline{U}_j}{\partial x_i} = -\frac{1}{\rho}\frac{\partial \bar{p}}{\partial \bar{x}_i} + v\frac{\partial^2 \overline{U}_i}{\partial x_i x_j} - \frac{\partial \overline{\grave{u}_i \grave{u}_j}}{\partial x_j} \tag{6}$$

where U_i and U_j indicates the velocity vectors in i and j directions, u_i and u_j is the mean velocity component in i and j directions, x_i and x_j is the Cartesian component of the length, and the $\overline{\grave{u}_i \grave{u}_j}$

indicates the Reynolds stresses. The directions can be written as cartesian axis such as $i = 1, 2, 3$. ρ indicates the density of air, p indicates the fluid pressure, and v indicates the fluid kinematic viscosity.

The simulation was conducted by employing the turbulence model into the Shear-stress Transport SST $k - \omega$ model which can compute the fluctuating velocity component through the computational domain [37], [38]. The SST $k - \omega$ is formulated by Eqs. (7) and (8) [22], [39]:

$$\frac{\partial}{\partial t}(\rho k) + \frac{\partial}{\partial x_i}(\rho k u_i) = \frac{\partial}{\partial x_j}\left[\Gamma_k \frac{\partial k}{\partial x_j}\right] + G_k - Y_k + S_k \tag{7}$$

$$\frac{\partial}{\partial t}(\rho \omega) + \frac{\partial}{\partial x_i}(\rho \omega u_i) = \frac{\partial}{\partial x_j}\left[\Gamma_\omega \frac{\partial \omega}{\partial x_j}\right] + G_\omega - Y_\omega + S_\omega \tag{8}$$

Γ_k and Γ_ω define the effective diffusivity which can be calculated by Eqs. (9) and (10):

$$\Gamma_k = \mu + \frac{\mu_t}{\sigma_k} \tag{9}$$

$$\Gamma_\omega = \mu + \frac{\mu_t}{\sigma_\omega} \tag{10}$$

where the G_k and G_ω indicate the generation of turbulence kinetic energy and ω resulting from the mean velocity gradients, Y_k and Y_ω indicate the k and ω dissipation, S_k and S_ω indicate the user-designed source terms.

The reference values that contain velocity, area, air density, etc., are estimated as the value for calculating the coefficient of moments (C_M). The methods are chosen as High Order Term Relaxation. The reported values are the moment coefficient with convergence criteria of 1×10^{-4} for residuals and the iterations are set into 1000 iterations until the convergence calculation reached. The coupled scheme is performed for pressure-velocity coupling. The spatial discretization gradient is least squares cell based. Then, other parameters are chosen such as the second order for pressure, second-order upwind for momentum, turbulent kinetic energy, and specific dissipation rate. Coughtrie et al. [40] declared that the separation and high adverse pressure gradient in the flow behavior through the motor surface can be predicted well.

3. Results and Discussion

3.1. Experimental result

Figure 8 presents a graphic of the blade number effect on (a) generator power and (b) tip speed ratio. **Figure 8a** shows the comparison between ASWT with 3 blades and 4 blades giving variations in generator power. At 1 m/s wind speed, both turbines generate power around 0-0,54 watt. The wind speed was increased which caused the power to increase. At 5 m/s, the 3 blades turbine generates more power around 158,5% than 4 blades turbine. Until the maximum wind speed at 7 m/s, the output power of 3 blades turbine always increases. **Figure 8b** shows the tip speed ratio (TSR) comparison of both turbines. Briefly, both turbines have significantly different TSRs which are 30-95% different at all variation wind speeds. The maximum TSR is 52,761 which was generated by ASWT with 3 blades at 7 m/s wind speed. These findings align with previous studies, such as those by Omid Salah Samiani et al. [41] which demonstrated that factors like opening angle, pitch, and rotational speed significantly influence ASWT performance. Their research resulted in an optimized design with a 27.72% efficiency increase, 7.94% thrust reduction, and a power coefficient of 0.2644 while operating at lower Tip Speed Ratios (TSR) to minimize noise.

To validate and contextualize these findings, comparisons with other studies are crucial. For instance, Bhattarai et al. reported a maximum power coefficient of 0.25 for ASWTs with 60° opening angles, which aligns with the trends observed in this study, where the 3 blades configuration achieved higher efficiency. Similarly, Rao et al. demonstrated that spiral blades outperform traditional aerofoil designs at low wind speeds, reinforcing the aerodynamic advantages seen in this research. The superior performance of the 3 blades configuration can be attributed to enhanced aerodynamic principles. The lower number of blades minimizes drag and allows undisturbed airflow through the turbine, reducing the blocking effect. This is consistent with flow dynamics theory, where fewer blades improve acceleration while maintaining efficient energy transfer from wind to rotational motion.

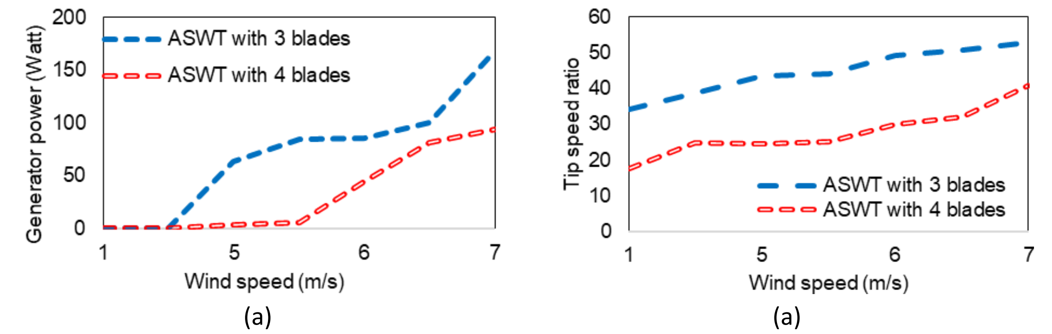

Figure 8. The effect of blade number on (a) generator power and (b) tip speed ratio

Wind turbine efficiency is obtained from the ratio of wind power and turbine power. The efficiency is represented in a 3D surface plot. **Figure 9** presents the 3D surface plot of turbine efficiency with (a) 3 blades and (b) 4 blades. The 3-blade turbine can give 83,49% of maximum efficiency than the 4-blade turbine which is only 31,76%.

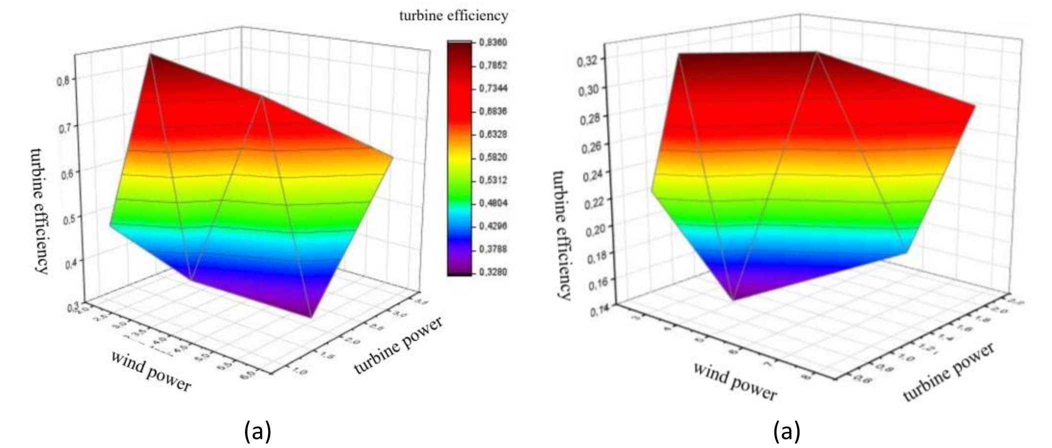

Figure 9. The 3D surface plot of turbine efficiency with (a) 3 blades and (b) 4 blades

3.2. Simulation result

To compare the speed pathline around the ASWT surface obtained from the CFD simulations. **Figure 10** shows the results at a constant wind speed of 7 m/s. These comparisons have been made using the pathline view in the CFD post-processing. The solution bar represents the color line in velocity magnitude. The red color indicates an increase in airflow velocity while the dark blue color shows a decrease in airflow velocity. The velocity magnitude can be seen in **Table 2**. The increase in airflow speed is because the air is captured by the turbine spiral blades so that it gathers in the center of the rotor with a subsequent increase in speed, which is shown by the red pathline speed. In addition, the highest speed region appears near the tip of the turbine rotor, while the lowest speed region appears behind the hub, resulting in turbulence in this area and reverse flow shown in the vector direction back to the inlet, this is caused by the effect of forming the direction of air flow after passing through the spiral turbine blade periodically. The same thing also happened in the research conducted by Song [16], namely the appearance of turbulent flow in the area behind the blade.

Moreover, this paper investigates the changes in different parameters in terms of the coefficient of drag (C_D), coefficient of lift (C_L), and coefficient of moments (C_M). These investigations are conducted using CFD simulation. CFD performs the simulation and solves the flow governing equations around the turbine blade for each of two different ASWT designs in 7 m/s of wind speed. Then, the results of the number of blades $(n = 3 \; and \; 4)$ and the fixed-opening angle $(\theta = 65°)$ are discussed in **Table 2**, that shows the velocity magnitude, coefficients of drag (C_D), coefficient of lift (C_L), and coefficient of moments (C_M) for the ASWT with different blade configurations (n = 3 and n = 4). The simulation utilized a structured mesh with a size of 10 mm, chosen to optimize the trade-off between computational efficiency and simulation accuracy. The boundary conditions included a free-stream velocity of 10 m/s and a turbulence intensity of 5%, representing typical urban wind profiles.

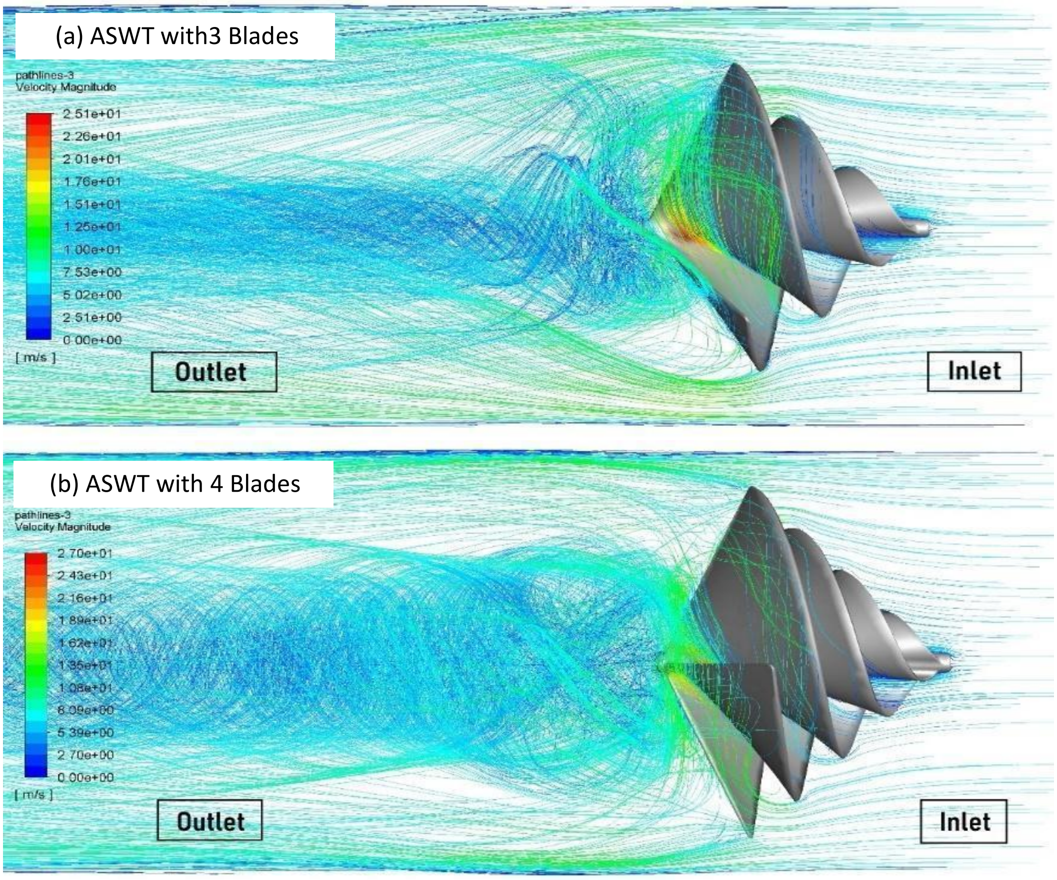

Figure 10. The speed pathline comparison around the ASWT with (a) 3 blades and (b) 4 blades

Table 2. The velocity magnitude

Number of blades	The velocity magnitude (m/s)	coefficient of lift (C_L)	coefficient of drag (C_D)	coefficient of moments (C_M)
$n = 3$	27.0	0.27074	-2.1758	0.6127
$n = 4$	25.1	0.12544	-1.9286	0.5309

The drag force is influenced by the surface area and the pressure differential across the blades. The smallest C_D value and the highest C_L value is for the ASWT with 3 blades. In an ASWT with 3 blades, undisturbed free flow can pass through the blades more easily than with 4 blades which mean the air blocking effect is minimum. The fewer blades present, the less interaction there is between the wake generated by one blade and the oncoming airflow for the other blades. This reduces wake interference, ensuring a more consistent and laminar airflow over each blade, which is essential for maintaining higher aerodynamic efficiency. A positive C_D value means drag, and a negative C_D value means acceleration. It can be concluded that the spiral blade with 3 blades has the best acceleration because the C_D value is the smallest. With three blades, the overall surface area in contact with the airflow is reduced compared to a four-blade configuration. This minimizes the drag force acting against the turbine and allows it to operate with greater acceleration, as reflected in the negative C_D value for the three-blade configuration.

The coefficient of moments (C_M) represents the aerodynamic moment created by the blades about the turbine's rotational axis. The magnitude of the C_M value tends to increase as the number of blades decreases. A small coefficient of moment (C_M) value means that the rotary torque produced by the turbine is small, while a large coefficient of moment (C_M) value means that the rotary torque produced by the turbine is large, so the turbine has good performance. For the 3 blades configuration, the larger C_M value (0.6127) indicates that this design generates significantly more torque compared to the 4 blades configuration (0.5309). This higher torque reflects better turbine performance, as it enables the rotor to spin more powerfully and efficiently, allowing for greater energy extraction from the wind. In contrast, the 4-blade configuration, with a lower C_M value, produces less torque, which may result in reduced energy output. However, this lower torque could provide certain operational advantages, such as reduced vibrations and potentially smoother rotation, making it more suitable for scenarios where stability and structural integrity are prioritized over maximum energy efficiency. This trade-off highlights the importance of selecting a configuration that balances torque, energy generation, and operational stability based on specific application requirements.

In essence, the superior performance of the three-blade turbine is attributed to better flow management, lower drag, and higher aerodynamic efficiency. The design minimizes the interference effects and energy losses associated with turbulence and drag while maximizing lift and torque generation. These aerodynamic advantages make the 3 blades configuration the optimal choice for achieving high performance in the ASWT.

4. Conclusion

Archimedes Spiral Wind Turbine (ASWT) is a unique blade design turbine that is categorized as a low-speed axial flow turbine. This turbine can convert electric power from wind energy as an environmentally friendly energy source. Many societies in urban areas have utilized this turbine because of its simple design and easy to manufacture. In this current study, experimental work was conducted to obtain the generated power by investigating the effect of blade number. To validate the aerodynamics of both ASWT designs, the simulation was performed. Some findings appeared from this study that the blade number significantly affected the generator power which the 3 blades can generate 158,5% of power than the turbine with more than 3 blades. The tip speed ratio (TSR) also showed 30-95% differences between both turbines, and the 3 blades turbine has high TSR that causes the efficiency increase. The simulation results showed that the blade number affected the air flow after passing through the spiral turbine blade which caused different aerodynamic performances of each turbine. The results of this study highlight the potential of the 3-blade ASWT design for real-world applications, particularly in urban settings where compact, efficient, and environmentally friendly renewable energy solutions are needed. The high efficiency and power generation capabilities make this design suitable for small-scale electricity generation in residential areas, rooftop installations, and off-grid energy systems. Future research should focus on optimizing the ASWT design further by exploring variations in blade geometry, materials, and structural reinforcements to enhance durability and performance under diverse environmental conditions. Additionally, integrating hybrid renewable energy systems with ASWTs and investigating their performance in varying wind profiles could provide more comprehensive insights for broader applications.

Acknowledgments

The author thanks reviewers and proofreaders, as well as technicians who help prepare equipment set-ups and students who assist in data collection.

Authors' Declaration

Authors' contributions and responsibilities - The authors made substantial contributions to the conception and design of the study. The authors took responsibility for data analysis, interpretation, and discussion of results. The authors read and approved the final manuscript.

Funding – No funding information from the authors.

Availability of data and materials - All data is available from the authors.

Competing interests - The authors declare no competing interest.

Additional information – No additional information from the authors.

References

[1] B. M. Opeyemi, "Path to sustainable energy consumption: The possibility of substituting renewable energy for non-renewable energy," *Energy*, vol. 228, no. 120519, 2021, doi: 10.1016/j.energy.2021.120519.

[2] Amir shasavari; Azadeh Karimi ; Morteza Akbari; Mohammad Alizadeh Noughani, "Environmental Impacts and Social Cost of Non-Renewable and Renewable Energy Sources:

A Comprehensive Review," *Journal of Renewable Energy and Environment*, vol. 11, no. 1, 2024, doi: 10.30501/jree.2023.382598.1545.

[3] J. S. Yadav, K. Shirisha, and C. M. Rao, "Mini cold storage using the parabolic solar trough: An appropriate technology for perishable agricultural product," *Mechanical Engineering for Society and Industry*, vol. 2, no. 1, pp. 35–41, 2022, doi: 10.31603/mesi.6368.

[4] S. Susilawati, A. Nugraha, A. S. S. Buchori, S. Rahayu, F. Fathurohman, and O. Yudiyanto, "Design and implementation of automatic fish feeder (AFF) using microcontroller powered by solar cell: A Contribution to the fish farmers," *Mechanical Engineering for Society and Industry*, vol. 3, no. 1, pp. 47–53, Mar. 2023, doi: 10.31603/mesi.8276.

[5] R. A. Rahman, S. Sulistyo, M. S. K. T. S. Utomo, D. Ragil, and B. M. Suyitno, "Experimental evaluation on the power characteristic of direct-photovoltaic charging for thermal storage equipment," *Mechanical Engineering for Society and Industry*, vol. 4, no. 1, pp. 115–122, Jul. 2024, doi: 10.31603/mesi.11493.

[6] Y. D. Herlambang *et al.*, "Study on Solar Powered Electric Vehicle with Thermal Management Systems on the Electrical Device Performance," *Automotive Experiences*, vol. 7, no. 1, pp. 18–27, 2024, doi: 10.31603/ae.10506.

[7] A. Supardi and A. H. F. Anisa, "Design of solar-powered automatic plant watering based on Internet of Things," *BIS Energy and Engineering*, vol. 1, pp. V124026–V124026, 2024, doi: 10.31603/biseeng.83.

[8] A. Chaudhuri, R. Datta, M. P. Kumar, J. P. Davim, and S. Pramanik, "Energy Conversion Strategies for Wind Energy System: Electrical, Mechanical and Material Aspects," *Materials*, vol. 15, no. 3, pp. 1–34, 2022, doi: 10.3390/ma15031232.

[9] H. M. Boulouiha, A. Allali, and M. Denai, "Chapter Nine - Grid Integration of Wind Energy Systems: Control Design, Stability, and Power Quality Issues," M. G. Rasul, A. kalam Azad, and S. C. B. T.-C. E. for S. D. Sharma, Eds. Academic Press, 2017, pp. 239–335.

[10] A. A. Afif, P. Wulandari, and A. Syahriar, "CFD analysis of vertical axis wind turbine using ansys fluent," *Journal of Physics: Conference Series*, vol. 1517, no. 1, 2020, doi: 10.1088/1742-6596/1517/1/012062.

[11] M. Kamran, *Planning and modeling of wind energy systems*. Elsevier, 2023.

[12] M. A. Al-Rawajfeh and M. R. Gomaa, "Comparison between horizontal and vertical axis wind turbine," *International Journal of Applied Power Engineering*, vol. 12, no. 1, pp. 13–23, 2023, doi: 10.11591/ijape.v12.i1.pp13-23.

[13] E. Achdi, B. F. T. Kiono, S. H. Winoto, and M. Facta, "Improving cross-axis wind turbine performance: A Lab-scale investigation of rotor size and blades number," *Mechanical Engineering for Society and Industry*, vol. 4, no. 1, pp. 82–91, Jul. 2024, doi: 10.31603/mesi.10837.

[14] Y. Dai, Z. Deng, B. Li, L. Zhong, and J. Wang, "Study on the Relationship between Structural Aspects and Aerodynamic Characteristics of Archimedes Spiral Wind Turbines," *Fluid Dynamics & Materials Processing*, vol. 20, no. 7, pp. 1517–1537, 2024, doi: 10.32604/fdmp.2024.046828.

[15] N. K. P, "Design and Flow Simulation Of An Archimedean Spiral-Type Wind Turbine Blade For Determining Velocity And Pressure Profile," *EPRA International Journal of Multidisciplinary Research (IJMR)*, vol. 7, no. 12, pp. 198–210, 2021, doi: 10.36713/epra2013.

[16] Y. K. Ke Song, Huiting Huan, "Aerodynamic Performance and Wake Characteristics Analysis," *Energies*, vol. 16, no. 1, 2023, doi: 10.3390/en16010385.

[17] A. S. Ansari, T. Hussain, A. Hussain, and I. Ali, "Efficiency Analysis of Archimedes Wind Turbine Using CFD Technique," *International Journal of Scientific & Engineering Research*, vol. 12, no. 3, pp. 51–55, 2021.

[18] K. C. Kim, H. S. Ji, Y. K. Kim, Q. Lu, J. H. Baek, and R. Mieremet, "Experimental and numerical study of the aerodynamic characteristics of an archimedes spiral wind turbine blade," *Energies*, vol. 7, no. 12, pp. 7893–7914, 2014, doi: 10.3390/en7127893.

[19] M. Casini, "Small Vertical Axis Wind Turbines for Energy Efficiency of Buildings," *Journal of Clean Energy Technologies*, vol. 4, no. 1, pp. 56–65, 2015, doi: 10.7763/jocet.2016.v4.254.

[20] Abdelaziz G. Refaie, H. S. A. Hameed, Y. A. A. Mohamed A.A. Nawar, and M. H. Mohamed, "Comparative investigation of the aerodynamic performance for several Shrouded

Archimedes Spiral Wind Turbines," *Energy*, vol. 239, 2022, doi: 10.1016/j.energy.2021.122295.

[21] H. Hamid and R. M. Abd El Maksoud, "A comparative examination of the aerodynamic performance of various seashell-shaped wind turbines," *Heliyon*, vol. 9, no. 6, p. e17036, 2023, doi: 10.1016/j.heliyon.2023.e17036.

[22] A. M. Kamal, M. A. A. Nawar, Y. A. Attai, and M. H. Mohamed, "Blade design effect on Archimedes Spiral Wind Turbine performance: Experimental and numerical evaluations," *Energy*, vol. 250, p. 123892, 2022, doi: 10.1016/j.energy.2022.123892.

[23] A. I. Siswantara, Warjito, Budiarso, R. Harmadi, M. H. Gumelar, and D. Adanta, "Investigation of the α angle's effect on the performance of an Archimedes turbine," *Energy Procedia*, vol. 156, pp. 458–462, 2019, doi: 10.1016/j.egypro.2018.11.084.

[24] A. Bhattarai, H. P. Bashyal, S. Sapkota, and U. Nepal, "Design, CFD Analysis and Modelling of Archimedean-Spiral type Wind Turbine," no. January 2016, pp. 1–83, 2019.

[25] E. H. Herraprastanti and W. Agung Saputro, "Simulation of Opening Angle of Archimedes Wind Turbine Design Based on the Fibonacci Series," *International Journal of Engineering, Science and Information Technology*, vol. 2, no. 1, pp. 50–57, 2021, doi: 10.52088/ijesty.v2i1.192.

[26] A. M. Labib, A. F. A. Gawad, and M. M. Nasseif, "Effect of Blade Angle on Aerodynamic Performance of Archimedes Spiral Wind Turbine," *Journal of Advanced Research in Fluid Mechanics and Thermal Sciences*, vol. 78, no. 1, pp. 122–136, 2020, doi: 10.37934/ARFMTS.78.1.122136.

[27] M. H. M. Mohamed A.A. Nawar, H.S. Abdel Hameed, A. Ramadan, Youssef A. Attai, "Experimental and numerical investigations of the blade design effect on Archimedes Spiral Wind Turbine performance," *Energy*, vol. 223, no. 120051, 2021, doi: 10.1016/j.energy.2021.120051.

[28] A. Khan, A. Khattak, A. Ulasyar, K. Imran, and M. A. Munir, "Investigation of Archimedean Screw Turbine for Optimal Power Output by Varying Number of Blades," *1st International Conference on Electrical, Communication and Computer Engineering, ICECCE 2019*, no. July, pp. 1–6, 2019, doi: 10.1109/ICECCE47252.2019.8940654.

[29] K. Kashyap, R. Thakur, R. Kumar, and S. Kumar, "Feasibility analysis for conversion of existing traditional watermills in Western Himalayan region of India to micro-hydropower plants using a low head Archimedes screw turbine for rural electrification," *International Journal of Ambient Energy*, vol. 43, no. 1, pp. 7463–7473, 2022, doi: 10.1080/01430750.2022.2068056.

[30] C. E. S. Juan Manuel De Egea Juvinel , Diego P. Pinto Roa, "Structural and Shape Optimization in Aerodynamic Airfoil Performance: A Literature Review," *Preprints*, 2023, doi: 10.20944/preprints202307.0807.

[31] A. T. Mustafa; and H. A. Jaleel, "A comparison study between Archimedes spiral turbine and propeller turbine with wind attack angle effect," *AIP Conference Proceedings*, vol. 1, 2020.

[32] S. Rao, K. Shanmukesh, M. K. Naidu, and Praveen Kalla, "Design and Analysis of Archimedes Aero-Foil Wind Turbine Blade for Light and Moderate Wind Speeds," *International Journal on Recent Technologies in Mechanical and Electrical Engineering (IJRMEE)*, vol. 5, no. August, pp. 1–5, 2018.

[33] Conrado Ostia, J. M. Martinez, and K. T. Coderes, "Development of a Dual Wind Turbines using the Savonius and Archimedes Spiral Principle," *EEE 10th international conference on humanoid, nanotechnology, information technology, communication and control, Environment and Management (HNICEM)*, pp. 1–5, 2018.

[34] K. Kashyap, R. Thakur, S. Kumar, and Rajkumar, "Identification of archimedes screw turbine for efficient conversion of traditional water mills (gharats) into micro hydro-power stations in Western Himalayan Regions of India: An experimental analysis," *International Journal of Renewable Energy Research*, vol. 10, no. 3, pp. 1451–1463, 2020, doi: 10.20508/ijrer.v10i3.11176.g8020.

[35] N. Kumar Thakur, R. Thakur, K. Kashyap, and B. Goel, "Efficiency enhancement in Archimedes screw turbine by varying different input parameters - An experimental study," *Materials Today: Proceedings*, vol. 52, pp. 1161–1167, 2022, doi: 10.1016/j.matpr.2021.11.020.

[36] M. D. Lee and P. S. Lee, "Modelling the Energy Extraction from Low-Velocity Stream Water by

Small Scale Archimedes Screw Turbine," *Journal of King Saud University - Engineering Sciences*, vol. 35, no. 5, pp. 319–326, 2023, doi: 10.1016/j.jksues.2021.04.006.

[37] A. Rezaeiha, H. Montazeri, and B. Blocken, "On the accuracy of turbulence models for CFD simulations of vertical axis wind turbines," *Energy*, vol. 180, pp. 838–857, 2019, doi: 10.1016/j.energy.2019.05.053.

[38] W. Huang, W. Liu, S. Li, and Z. Xia, "Influences of the turbulence model and the slot width on the transverse slot injection flow field in supersonic flows," *Acta Astronautica*, vol. 73, pp. 1–9, 2012, doi: 10.1016/j.actaastro.2011.12.003.

[39] B. R. Munson, D. F. Young, and T. H. Okiishi, "Fundamentals of fluid mechanics," 1994, doi: 10.1201/b11709-7.

[40] A. R. Coughtrie, D. J. Borman, and P. A. Sleigh, "Effects of turbulence modelling on prediction of flow characteristics in a bench-scale anaerobic gas-lift digester," *Bioresour Technol*, vol. 138, pp. 297–306, 2013, doi: 10.1016/j.biortech.2013.03.162.

[41] O. S. Samiani and M. Boroushaki, "Optimal design of Archimedes Wind Turbine using genetic algorithm," vol. 314, no. November 2024, 2025.

!

An update of this article is available in Vol. 5 No. 1 (2025), pp. 286-287
doi: 10.31603/mesi.13996